Towards Lane-Keeping Electronic Stability Control for Road-Vehicles ⋆

Kristoffer Lundahl * **Björn Olofsson** ** **Karl Berntorp** ** **Jan Åslund** *
Lars Nielsen *

* *Department of Electrical Engineering, Linköping University, SE–581 83 Linköping, Sweden,* firstname.lastname@liu.se.
** *Department of Automatic Control, Lund University, SE–221 00 Lund, Sweden,* firstname.lastname@control.lth.se.

Abstract: The emerging new idea of lane-keeping electronic stability control is investigated. In a critical situation, such as entering a road curve at excessive speed, the optimal behavior may differ from the behavior of traditional ESC, for example, by prioritizing braking over steering response. The important question that naturally arises is if this has a significant effect on safety. The main contribution here is to give a method for some first quantitative measures of this. It is based on optimal control, applied to a double-track chassis model with wheel dynamics and high-fidelity tire-force modeling. The severity of accidents grows with the square of the kinetic energy for high velocities, so using kinetic energy as a measure will at least not overestimate the usefulness of the new safety system principle. The main result is that the safety gain is significant compared to traditional approaches based on yaw rotation, for several situations and different road-condition parameters.

1. INTRODUCTION

New possibilities for electronic stability control systems (ESC) (Isermann, 2006; Bosch, 2011; Rajamani, 2006) of vehicles are now emerging, and the reason is increased situation awareness due to preview sensors like cameras, radar, and satellite positioning systems (such as GPS). With the availability of individual braking of each wheel, possibilities arise for a spectrum of new systems, for example, collision avoidance or collision mitigation (Chakraborty et al., 2013).

One highly critical situation is if a vehicle leaves its lane, that is, enters the lane of opposing traffic or exits the road. Already now there exists lane-departure warning (LDW) systems (Kim and Oh, 2003), which are aware of such situations and alert the driver in case of danger. This information is also deployed in lane-keeping systems, which during normal driving actively corrects a driver drifting out of lane with superimposed mild control (Ali, 2012). A next step would be to utilize this information in more severe situations, such as in (Ali et al., 2013) and (Benine-Neto, 2011), leading to systems we here refer to as lane-keeping ESC.

A number of interesting questions immediately arise, both around what the resulting vehicle behavior would be and how significant it would be in terms of increased safety for the driver and passengers. Regarding vehicle behavior, it is interesting to compare traditional ESC and optimal lane-keeping ESC in critical situations, and a typical situation to study is overspeed when entering a curve. Hence, this paper aims to quantify the performance gains in terms of the highest possible entry speed while staying in lane, when also trying to maintain vehicle controllability.

⋆ This work has been supported by ELLIIT, the Strategic Area for ICT research, funded by the Swedish Government. B. Olofsson and K. Berntorp are members of the LCCC Linnaeus Center at Lund University, supported by the Swedish Research Council.

1.1 Kinetic Energy as Severity Measure

Quantifying the level of safety and severity of critical situations leading to collision is complex, but to get a first grasp kinetic energy is a reasonable measure. The kinetic energy is proportional to the square of the velocity v, and thus an increase in velocity Δv results in increased kinetic energy. In a crash the kinetic energy has to be absorbed, and more absorbed kinetic energy implies that more damage will be caused. In (Jansson, 2005) it is stated that the probability of fatality is proportional to $(\Delta v)^4$, up to a certain maximum velocity. The velocity interval where this is valid is also bounded below and the reason is that cars are built to handle reasonable amounts of damage, and safety belts and airbags protect driver and passengers up to some limit. Therefore, using kinetic energy as a measure will at least not overestimate the usefulness of a new system that can handle cases where the vehicle enters maneuvering situations with critically high velocities.

1.2 Contribution and Outline

The main contribution in this paper is that we address the questions raised in the previous subsections with a quantitative method. A first major step doing so is to devise a method of investigation. A closely related study was presented in (Ali et al., 2013), where a lane-keeping ESC is compared to traditional ESC. Their proposed system consists of an MPC controller, essentially preventing the vehicle from entering the critical operating regions when initiating a corner with excessive speed. In a similar context, others have studied optimal behavior in a curve using a similar setup as we do, for example, (Sundström et al., 2010) and (Andreasson, 2009). In the two referred studies, wheel dynamics are neglected and longitudinal force is used directly as input in a simplified tire model. We are including wheel dynamics and comprehensive tire-force modeling. Moreover, the problem of lane keeping is formulated as

an optimization problem for each of the considered ESC configurations, with the lane borders as boundary conditions in the optimization. The major questions to analyze in the results are whether braking all wheels and then steer should be prioritized, or if braking wheels on one side to create a turning moment inducing early rotation of the vehicle is more beneficial. The particular aspect to consider here is the effect such differences in strategy has on kinetic energy.

This paper is outlined as follows. In Section 2 the preliminaries of the study are presented and the method of investigation is defined. The employed chassis and tire modeling is described in Section 3. In Section 4, the optimal control problem for lane-keeping in a curve situation is defined. The results are presented in Section 5 and they are subsequently discussed in Section 6. Finally, conclusions are given in Section 7.

2. METHOD

As mentioned above, there are previous studies comparing different *optimal* solutions for various actuator configurations (Sundström et al., 2010; Andreasson, 2009). However, to our knowledge, there are no previous comparisons to judge the significance of different behaviors compared to traditional control strategies including yaw-moment regulation, and a reason is presumably that it is not evident how to do so. A complete comparison is out of reach since it would require complete implementations of both, including a state-of-the-art ESC system and a proper driver model. The outcome would then be heavily dependent on the properties of these, and especially the lane-keeping skills of the driver model. However, the following approach should give a reasonable first estimate. The characteristics of the traditional ESC, which we denote as T-ESC, is to control yaw rate and body slip towards reference values, calculated from the driver steering input. This control is achieved by generating a yaw moment, around the vertical axis of the vehicle, by braking individual wheels (Bosch, 2011). Given a desired moment, the optimal braking strategy is to apply braking on both wheels at one side, distributed between front and rear depending on the current circumstances (Tøndel and Johansen, 2005; Johansen, 2006).

In order to investigate the full potential of the control strategies used in T-ESC, the best possible steering input together with an optimal braking distribution of the wheels on one side is considered. The studied maneuver is a left-hand turn initiated with excessive speed. In this situation the vehicle is subject to understeering, and a counterclockwise yaw-moment is therefore desired by the T-ESC scheme. To achieve this moment with an optimal braking distribution, the wheels on the left side are the only ones to be actuated according to the statements above. It is clear that such a strategy would overestimate the best behavior achievable with implementations of ESC systems today, since the driver influence is neglected and the braking and steering in traditional ESC are coupled via the reference model, and thus they are not free control variables. Such a vehicle with optimal braking on the left side in combination with an optimal steering-wheel input is one of the two vehicles used in the comparison. This vehicle will be labeled UBT-ESC for upper-bound traditional ESC. Given the preconditions for the different systems, the safety potential for UBT-ESC is strictly higher than for T-ESC.

The other configuration in the comparison will be able to brake all wheels individually and to steer optimally, and is here called optimal lane-keeping ESC, denoted OLK-ESC. The interesting research question is to investigate if there are any principle differences in behavior, and the maximum velocities that can be handled when over-speeding in a curve. Regarding behavior, the question is whether the vehicle makes a different tradeoff between yaw rate, side slip, and lane keeping. The fundamental aspect here is to investigate if the different strategies exhibit any significant improvements of safety. This gives a first engineering value for the potential of the different approach, which is highly valuable.

3. MODELING

We use a double-track model with roll and pitch dynamics and both longitudinal and lateral load transfer. Motivated by an ESC-system perspective in the study performed, it is essential to model the individual tire forces and also to incorporate load transfer effects, heavily influencing the available braking capacity (Lundahl et al., 2013). The chassis model has five degrees of freedom, and is illustrated in Figure 1. The vehicle chassis inertias in the roll, pitch, and yaw directions are I_{xx}, I_{yy}, and I_{zz}, respectively. Moreover, the distance from the center of mass to the road in steady state is denoted h. The complete derivation and dynamic equations for the model are omitted here because of space limitations; for the details we refer to (Berntorp, 2013). The suspension system is modeled as a rotational spring-damper system. Consequently, the moment τ_ϕ produced by the suspension system in the roll direction is given by

$$\tau_\phi = (K_{\phi,f} + K_{\phi,r})\phi + (D_{\phi,f} + D_{\phi,r})\dot{\phi}, \tag{1}$$

where ϕ is the roll angle, and correspondingly for τ_θ in the pitch direction according to

$$\tau_\theta = K_\theta \theta + D_\theta \dot{\theta}, \tag{2}$$

where θ is the pitch angle. In (1) and (2), K and D are model parameters for the stiffness and damping. The dynamic equations for the longitudinal load transfer are given by

$$(F_{z,1} + F_{z,2})l_f - (F_{z,3} + F_{z,4})l_r = K_\theta \theta + D_\theta \dot{\theta}, \quad \sum_{i=1}^{4} F_{z,i} = mg, \tag{3}$$

where $F_{z,i}$ denote the time-dependent normal forces, m is the vehicle mass, g is the constant of gravity, and l_f, l_r are defined as in Figure 1. The lateral load transfer is determined by the relations

$$-w(F_{z,1} - F_{z,2}) = K_{\phi,f}\phi + D_{\phi,f}\dot{\phi}, \tag{4}$$

$$-w(F_{z,3} - F_{z,4}) = K_{\phi,r}\phi + D_{\phi,r}\dot{\phi}, \tag{5}$$

where w is the half-track width, see Figure 1.

3.1 Wheel and Tire Modeling

The slip angles α_i and slip ratios κ_i are defined as in (Pacejka, 2006):

$$\dot{\alpha}_i \frac{\sigma}{v_{x,i}} + \alpha_i = -\arctan\left(\frac{v_{y,i}}{v_{x,i}}\right), \tag{6}$$

$$\kappa_i = \frac{R_w\omega_i - v_{x,i}}{v_{x,i}}, \; i \in \{1,2,3,4\}, \tag{7}$$

where σ is the relaxation length, R_w is the wheel radius, ω_i is the wheel angular velocity for wheel i, and $v_{y,i}$ and $v_{x,i}$ are the lateral and longitudinal wheel velocities for wheel i with respect to an inertial system, expressed in the coordinate system

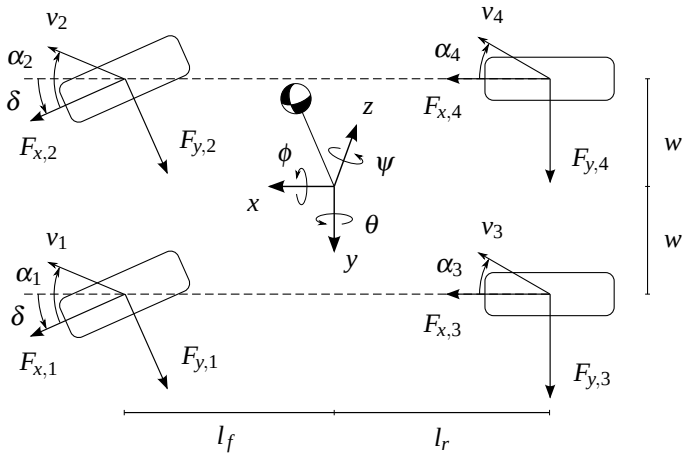

Fig. 1. The double-track model, with roll and pitch dynamics.

of the wheel. Note that Figure 1 illustrates the static slip angles, describing a pure geometric relation, compared to the dynamic relation in (6). The wheel dynamics are given by

$$T_i - I_w\dot{\omega}_i - F_{x,i}R_w = 0\ , \quad i \in \{1,2,3,4\}. \tag{8}$$

Here, T_i is the drive/brake torque and I_w is the wheel inertia. First-order dynamics are introduced for T_i according to

$$\dot{T}_i\gamma_T + T_i = T_{u,i}, \tag{9}$$

where $T_{u,i}$ is the control signal and γ_T a time constant.

The nominal tire forces—that is, the forces under pure slip conditions—are computed with the Magic Formula model [1] (Pacejka, 2006), given by

$$F_{x0,i} = \mu_{x,i}F_{z,i}\sin(C_{x,i}\text{atan}(B_{x,i}\kappa_i - E_{x,i}(B_{x,i}\kappa_i - \text{atan}B_{x,i}\kappa_i))), \tag{10}$$

$$F_{y0,i} = \mu_{y,i}F_{z,i}\sin(C_{y,i}\text{atan}(B_{y,i}\alpha_i - E_{y,i}(B_{y,i}\alpha_i - \text{atan}B_{y,i}\alpha_i))), \tag{11}$$

for each wheel i, $i \in \{1,2,3,4\}$. In (10)–(11), μ_x and μ_y are the friction coefficients and B, C, and E are model parameters. To model combined slip we use the empirically verified approach described in (Pacejka, 2006), where the nominal forces (10)–(11) are scaled with weighting functions $G_{x\alpha,i}$ and $G_{y\kappa,i}$, which depend on α and κ. The relations in the longitudinal direction are

$$H_{x\alpha,i} = B_{x1,i}\cos(\text{atan}(B_{x2,i}\kappa_i)), \tag{12}$$

$$G_{x\alpha,i} = \cos(C_{x\alpha,i}\text{atan}(H_{x\alpha,i}\alpha_i)), \tag{13}$$

$$F_{x,i} = F_{x0,i}G_{x\alpha,i},\ i \in \{1,2,3,4\}, \tag{14}$$

and the relations in the lateral direction are given by

$$H_{y\kappa,i} = B_{y1,i}\cos(\text{atan}(B_{y2,i}\alpha_i)), \tag{15}$$

$$G_{y\kappa,i} = \cos(C_{y\kappa,i}\text{atan}(H_{y\kappa,i}\kappa_i)), \tag{16}$$

$$F_{y,i} = F_{y0,i}G_{y\kappa,i},\ i \in \{1,2,3,4\}, \tag{17}$$

where B and C are model parameters. The vehicle model parameters used in this paper are shown in Table 1 and the tire model parameters in Table 2.

4. OPTIMAL CONTROL PROBLEM

The chassis and tire model presented in the previous section is formulated as a differential-algebraic equation system according to $\dot{x}(t) = G(x(t),y(t),u(t))$, where x is the state vector, y is the algebraic variables vector, and u is the input signal vector. The time dependency of the variables will be implicit in the rest of the paper. The wheel-torque control signals, $T_u = (T_{u,1}\ T_{u,2}\ T_{u,3}\ T_{u,4})$, as well as the steer angle δ of the front wheels are considered as inputs. For simplicity we assume that the front wheels have the same steer angle. In the case with braking only on the left wheels, that is, UBT-ESC, it is required that $T_{u,2} = T_{u,4} = 0$. Further, the tire-force model is written as the equation system $h(x,y,u) = 0$. The chassis and tire dynamics are implemented using the modeling language Modelica (Modelica Association, 2014). The optimization problem is formulated over the time horizon $t \in [0,t_f]$, where the upper limit t_f on the time interval is free in the optimization. The optimization objective is to maximize the initial velocity v_0 when entering the curve. However, depending on the road geometry and the surroundings, it is sometimes not enough just to stay in lane; for example, when it leads to highly reduced vehicle controllability potentially resulting in other dangerous situations. Thus, the aim is also to avoid large body slip, which is defined as $\beta = \text{atan}(v_y/v_x)$, where v_x and v_y are the longitudinal and lateral velocities, respectively. This tradeoff is parametrized by using a weight η in the objective function. Accordingly, the dynamic optimization problem to be solved is written as:

[1] Also the tire modeling is essential in the study, since the resulting maneuvers are expected to utilize the maximum available tire forces. Hence, a model of comparably high complexity is motivated.

Table 1. Vehicle model parameters used in (1)–(8).

Notation	Value	Unit
l_f	1.3	m
l_r	1.5	m
w	0.8	m
m	2 100	kg
I_{xx}	765	kgm^2
I_{yy}	3 477	kgm^2
I_{zz}	3 900	kgm^2
R_w	0.3	m
I_w	4.0	kgm^2
γ_T	0.1	s
σ	0.3	m
g	9.82	ms^{-2}
h	0.5	m
$K_{\phi,f}, K_{\phi,r}$	89 000	Nm(rad)$^{-1}$
$D_{\phi,f}, D_{\phi,r}$	8 000	Nms(rad)$^{-1}$
K_θ	363 540	Nm(rad)$^{-1}$
D_θ	30 960	Nms(rad)$^{-1}$

Table 2. Tire model parameters in (10)–(17). The same parameters are used for both the left and the right wheel.

Notation	Front	Rear
μ_x	1.20	1.20
B_x	11.7	11.1
C_x	1.69	1.69
E_x	0.377	0.362
μ_y	0.935	0.961
B_y	8.86	9.30
C_y	1.19	1.19
E_y	−1.21	−1.11
B_{x1}	12.4	12.4
B_{x2}	−10.8	−10.8
$C_{x\alpha}$	1.09	1.09
B_{y1}	6.46	6.46
B_{y2}	4.20	4.20
$C_{y\kappa}$	1.08	1.08

$$\text{minimize} \quad -v_0 + \eta \int_0^{t_f} \beta^2 \mathrm{d}t \tag{18}$$

$$\text{subject to} \quad T_{u,i,\min} \le T_{u,i} \le T_{u,i,\max},\ i \in \{1,2,3,4\}, \tag{19}$$

$$|\delta| \le \delta_{\max}, \quad |\dot{\delta}| \le \dot{\delta}_{\max}, \tag{20}$$

$$x(0) = x_0, \quad x(t_f) = x_{t_f}, \tag{21}$$

$$f(X_p, Y_p) \le 0, \tag{22}$$

$$\dot{x} = G(x,y,u), \quad h(x,y,u) = 0, \tag{23}$$

where x_0 are the initial conditions for the differential states, x_{t_f} are the desired values at the final time $t = t_f$, and (X_p, Y_p) is the position of the center of gravity of the vehicle. In practice, the terminal conditions on the differential states are only applied to a subset of the model variables. Further, $f(X_p, Y_p)$ is a mathematical description of the road constraint for the center of gravity of the vehicle in the curve maneuver. This constraint is formulated as two circles with different radii in the XY-plane.

Since the primary objective of the safety system is to capture the first and most critical part of the situation, the terminal constraint is formulated as

$$\dot{e}(t_f) = 0.$$

Here e is the lateral deviation from the middle of the lane, defined as

$$e = \sqrt{X_p^2 + Y_p^2} - R, \tag{24}$$

where R is the mean radius of the curve. This terminal constraint implies that the vehicle has succeeded in avoiding going out-of-lane, and can either begin recovering from the critical situation, or immediately return control back to the driver.

The continuous-time optimal control problem (18)–(23) is solved using the open-source software JModelica.org (Åkesson et al., 2010), according to the method we presented in (Berntorp et al., 2013). In particular, the continuous-time optimization problem is discretized using direct collocation methods (Biegler et al., 2002), and the resulting discrete-time nonlinear optimization problem (NLP) is solved numerically using the state-of-the-art interior-point solver Ipopt (Wächter and Biegler, 2006). The Jacobian and the Hessian related to the problem are computed with numerical precision using automatic differentiation (Griewank, 2000), which is essential for robust convergence of the complex optimization problem at hand. For further details on the solution methodology, see (Berntorp et al., 2013).

5. RESULTS

The optimization problem (18)–(23) was solved for both UBT-ESC and OLK-ESC, in the circular-shaped curve with the lateral deviation (24) limited to $-1 \le e \le 1$ m. The maximum steer angle and maximum steer rate were set to $\delta_{\max} = 29$ deg and $\dot{\delta}_{\max} = 57$ deg/s, corresponding to reasonable physical and driver limitations. The vehicle was only allowed to utilize braking torques. The wheel torque limitations were set to $T_{u,i,\max} = 0$ and $T_{u,i,\min} = -7.4$ kNm. Here $T_{u,i,\min}$ was chosen sufficiently large, such that the tire force F_X is the main limiting factor for braking in the maneuver.

To evaluate the influence of the weighting factor η, the optimization problem was solved for different values of this parameter. In addition, to quantify the differences between UBT-ESC and OLK-ESC for different road conditions, the friction coefficients μ and the road-curvature radius R were also separately varied. The scaling of μ was done according to

Table 3. Initial velocity and maximum body-slip for different η, using $\gamma_\mu = 1$ and $R = 30$ m.

	UBT-ESC		OLK-ESC	
η	v_0 [km/h]	$\lvert\beta\rvert_{\max}$ [deg]	v_0 [km/h]	$\lvert\beta\rvert_{\max}$ [deg]
0	62.6	15	65.6	7.0
10	62.4	11	65.6	5.8
100	60.3	5.0	65.2	2.6
1000	55.6	2.1	64.5	1.0

Table 4. Initial velocity for reduced friction coefficients, using $\eta = 100$ and $R = 30$ m.

γ_μ	UBT-ESC, v_0 [km/h]	OLK-ESC, v_0 [km/h]	v_0-diff. [%]
1.00	60	65	8.2
0.90	57	62	8.1
0.80	54	58	7.9
0.70	51	55	7.4
0.60	47	51	7.3
0.50	43	46	7.3
0.40	38	41	7.4
0.30	33	36	7.7
0.20	27	29	8.4

$$\mu_{x,\text{scaled}} = \gamma_\mu \mu_x,$$
$$\mu_{y,\text{scaled}} = \gamma_\mu \mu_y,$$

where γ_μ is the scaling parameter. This is not an ideal representation for low-friction surfaces, see (Olofsson et al., 2013). However, it will give an indication of possible differences for various road surfaces. Solutions for all parametrization configurations of the optimization problem were typically found in 100–300 iterations, requiring approximately 200–300 s on a standard PC with an Intel Core i3 processor.

In Table 3, the initial velocity and the maximum body-slip, corresponding to different η-values, are summarized for the optimal solution obtained with UBT-ESC and OLK-ESC for $\gamma_\mu = 1$ and curve radius $R = 30$ m. For OLK-ESC, it is obvious that v_0 does not suffer from a larger η, that is, when penalizing body-slip more. For example, there is only a 1.7% loss in v_0 between $\eta = 0$ and $\eta = 1000$ for OLK-ESC. On the contrary, UBT-ESC exhibits a 11.2% reduction in v_0 for the corresponding weight difference. Also note that UBT-ESC results in considerably larger $|\beta|_{\max}$ for all values of η. Table 4 presents the initial velocity for UBT-ESC and OLK-ESC, when reducing the friction coefficient μ, using a weighting parameter of $\eta = 100$ and a road-curvature radius of $R = 30$ m. The table shows that the advantage of OLK-ESC can be seen to persist for the different friction levels, with very small variations, allowing an entry velocity of approximately 7–8% higher than UBT-ESC. The initial velocities resulting from different road-curvature radii are shown in Table 5. As for the friction-coefficient scaling, OLK-ESC results in a larger v_0 for all radii. Concerning entry velocity, the relative advantage of OLK-ESC is also consistent over the different road-curvatures, being about 7–9% compared to UBT-ESC.

In the following, the results achieved as the optimal solutions for UBT-ESC and OLK-ESC, using $\eta = 100$, $\gamma_\mu = 1$, and $R = 30$ m, are compared. In Figure 2, the geometric vehicle trajectories are presented. The start position was set to $(X_{p,0}, Y_{p,0}) = (30, 0)$ m, that is, in the lower right corner in the figure, with the vehicle heading in the tangential direction of the road. Figures 3 and 4 display the optimal trajectories of chassis variables and tire forces for UBT-ESC and OLK-ESC, in which

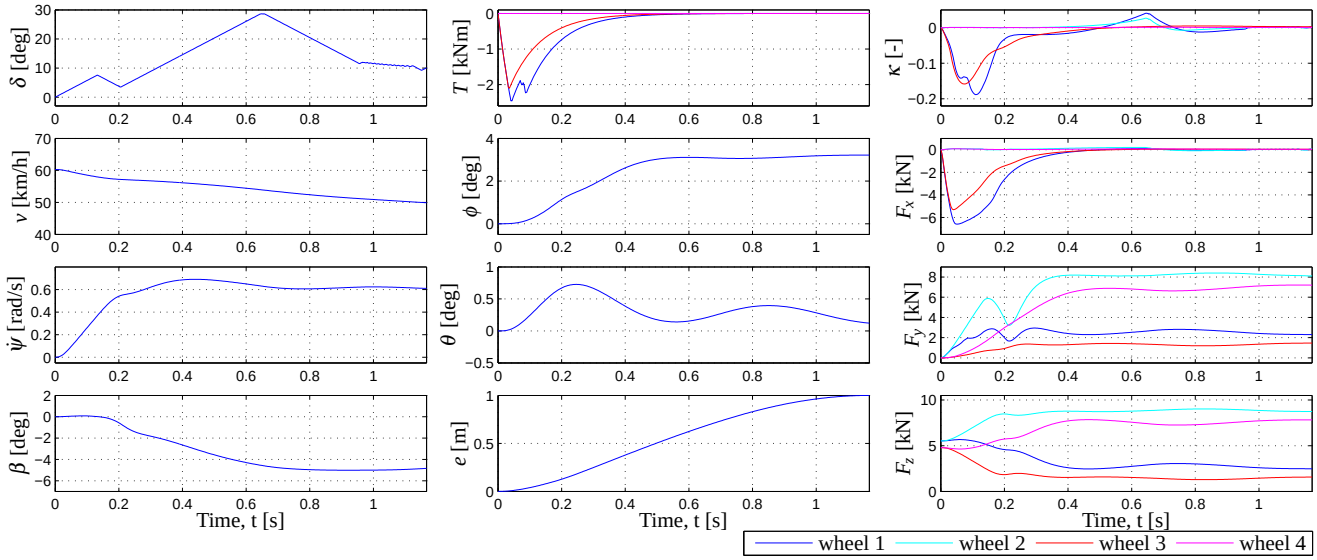

Fig. 3. Optimal control solutions obtained for UBT-ESC, with $\eta = 100$, $\gamma_\mu = 1$, and $R = 30$ m.

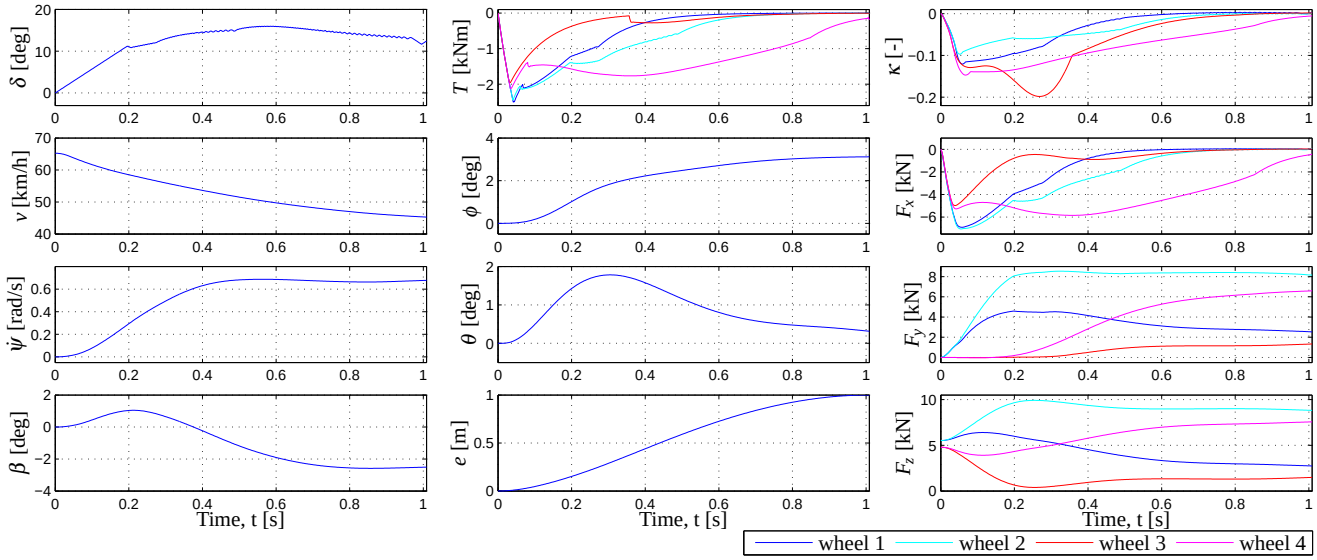

Fig. 4. Optimal control solutions obtained for OLK-ESC, with $\eta = 100$, $\gamma_\mu = 1$, and $R = 30$ m.

Table 5. Initial velocity for various road-curvature radii, using $\eta = 100$ and $\gamma_\mu = 1$.

R [m]	UBT-ESC, v_0 [km/h]	OLK-ESC, v_0 [km/h]	v_0-diff. [%]
10	38	42	9.3
15	46	49	8.4
20	52	55	7.6
25	56	61	7.7
30	60	65	8.2
40	68	74	8.2
50	75	81	7.8

the absolute velocity v is defined as

$$v = \sqrt{v_x^2 + v_y^2}.$$

Note that it is the wheel torque T_i, from (8), that is shown in Figures 3 and 4. Further, Figure 5 shows the sum of the longitudinal and lateral tire-forces F_X and F_Y, resolved in the road-surface plane. In addition, the yaw moment M_Z generated from the tire forces, that is, the moment about an axis orthogonal to the road, is visualized. These quantities are displayed as functions of the driven distance s to allow a more eligible comparison of the results from UBT-ESC and OLK-ESC. In Figure 6, the component of the yaw moment that is a result of the applied braking torques is shown. This moment is denoted ΔM and consists of the longitudinal braking forces F_x, as well as the reduction of the lateral forces resulting from the increased slip ratio κ during braking, and is defined as

$$\begin{aligned}\Delta M = &-F_{x,1}(w\cos\delta - l_f\sin\delta) + F_{x,2}(w\cos\delta + l_f\sin\delta)\\ &- F_{x,3}w + F_{x,4}w - (F_{y0,1} - F_{y,1})(l_f\cos\delta + w\sin\delta)\\ &- (F_{y0,2} - F_{y,2})(l_f\cos\delta - w\sin\delta) + (F_{y0,3} - F_{y,3})l_r\\ &+ (F_{y0,4} - F_{y,4})l_r.\end{aligned}$$

From Figures 2–6 it can be seen that OLK-ESC completes the maneuver both in shorter time and less driven distance. The time for executing the maneuver is for OLK-ESC $t_f = 1.0$ s and for UBT-ESC $t_f = 1.2$ s, and the total driven distance is $s_f = 14.8$ m and $s_f = 17.7$ m, respectively.

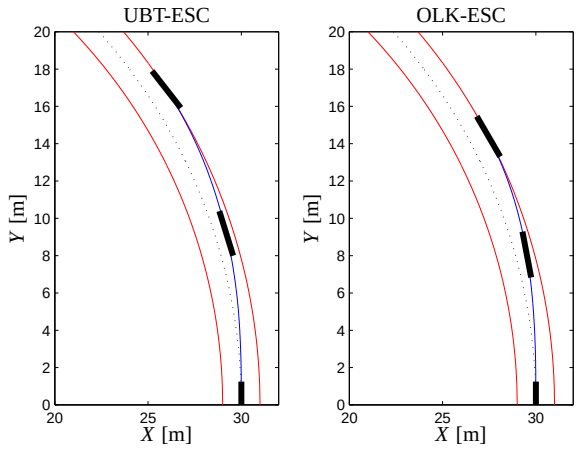

Fig. 2. Geometric trajectories for UBT-ESC and OLK-ESC, with $\eta = 100$, $\gamma_\mu = 1$, and $R = 30$ m. The black bars represent the vehicle position and heading direction for the initial, half-way, and final time-instant.

When analyzing the control strategies for UBT-ESC and OLK-ESC, seen in Figures 3 and 4, the most apparent difference is the emphasis on braking versus creating a yaw moment. UBT-ESC initially applies heavy braking at the left wheels, which subsequently is reduced as the normal forces F_z for these wheels decrease as a result of lateral load transfer. With this strategy, a positive yaw-moment contribution is always achieved, see ΔM in Figure 6, acting in the same direction as the total yaw moment, see M_Z in Figure 5.

For OLK-ESC, however, braking is applied throughout the whole maneuver, see T in Figure 4. Initially, a large braking effort is applied on all wheels, followed by reduced braking on all wheels except wheel 4. Because of the longitudinal and lateral load transfer, the normal load $F_{z,3}$ is significantly reduced. Hence, only small tire forces can be realized, and the braking is therefore rapidly decreased for this wheel, see T_3. For the front wheels, the braking is gradually reduced as the steer angle increases and the front lateral forces develop. Moreover, because of the lateral load transfer, larger tire forces can be utilized at the outer wheels (wheel 2 and 4), and a larger braking effort can thus be employed at these wheels. Notice that this will contribute to a negative ΔM (see Figure 6) counteracting the yaw moment M_Z in Figure 5. The differences between UBT-ESC and OLK-ESC in braking effort throughout the maneuver is also clearly seen in F_X, Figure 5. However, UBT-ESC leads to a solution with larger lateral forces F_Y (mainly around $s = 6$ m) and, in the initial phase, a larger yaw moment M_Z. Hence, OLK-ESC results in a strategy with more emphasis on braking, while sacrificing some of the cornering abilities in terms of lateral forces F_Y and yaw moment M_Z.

6. DISCUSSION

As an alternative to traditional ESC systems (T-ESC), whose maximum safety potential is captured by the system called UBT-ESC, we have considered an improved safety system principle, OLK-ESC, utilizing all wheels for braking and the situation awareness emerging in modern vehicles. The obtained results from a quantitative comparison based on optimal control using the UBT-ESC and OLK-ESC control principles exhibit several interesting differences. First, the control strategy observed for OLK-ESC in Section 5 differs considerably from

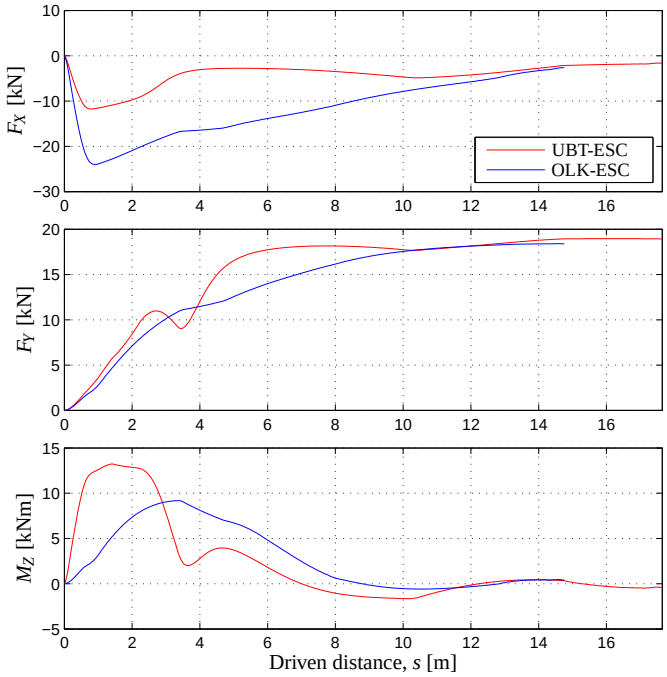

Fig. 5. Longitudinal force F_X, lateral force F_Y, and yaw moment M_Z, developed by the tires, illustrated as functions of the driven distance s.

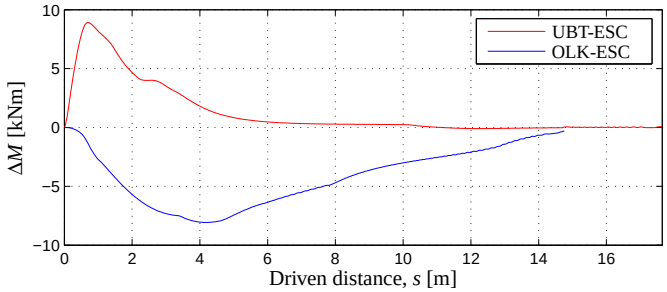

Fig. 6. The braking forces contribution to the yaw moment.

the approach of more traditional stability control incorporating yaw rotations. Regarding methodology, the most obvious is the heavy braking leading to decreased velocity (and thus kinetic energy), instead of focusing on applying an asymmetric braking behavior achieving a yaw moment such that the vehicle starts to rotate in the initial phase. A physical interpretation of this is that reduced kinetic energy makes it easier to stay in lane. Moreover, the fact that OLK-ESC favors braking to such extent that it generates a moment counteracting the yaw rotation is surprising (see Figure 6).

A series of optimal control problems was solved, where the maximum initial velocity was determined for different friction coefficients and curve radii (see Tables 4–5). It is clear that the OLK-ESC performs significantly better than UBT-ESC for all considered cases. The performance improvement over UBT-ESC that OLK-ESC can deliver in terms of higher entry speed is consistent regardless of friction coefficient and road-curvature radius. Only minor deviations are seen in the relative difference in initial velocity for the different situation parameters. The gain achieved with OLK-ESC is approximately 8%, when measured as increased initial velocity that can be handled. As mentioned in the introduction, it is to be noted that UBT-ESC determined the optimal combination of steering input and yaw

moment generation with full vehicle state and road information, which corresponds to the best achievable performance for this control principle in the given situation, but clearly overestimates the capabilities of traditional ESC approaches. Consequently, the safety performance increase from T-ESC to OLK-ESC in an implementation should be significant.

In Section 1, the kinetic energy was introduced as a measure of severity in impact situations. The kinetic energy is proportional to the square of the velocity; hence, reducing the vehicle velocity prior to a collision is essential. Based on the results achieved for OLK-ESC, with heavy initial braking, it is plausible that this system would be beneficial also from this perspective compared to traditional approaches.

Considering the promising results obtained for OLK-ESC in this paper, a natural question is the feasibility and implementation of its strategy. One option would be to employ direct onboard optimization, but with the computation times reported in Section 5 this is not possible to realize today. Nevertheless, with the current trend with decreasing computation times and increasing computing power in vehicles, the vision of implementation is there. Moreover, other approaches based on offline optimization (for example to the purpose of creating a library of optimal solutions parametrized for a few key variables) or approximation of parts of the vehicle model.

7. CONCLUSIONS

To study lane-keeping ESC, a quantitative method has been devised based on two vehicles employing two different safety-system principles, UBT-ESC and OLK-ESC. The dynamics are modeled using double-track models with load transfer, and with explicit modeling of wheel dynamics and tire-forces. The computational method used is optimal control with the lane borders as boundary conditions in the problem formulation. The results showed that initial full braking is advantageous compared to traditional ESC strategies resulting in yaw rotation. At the same time, reduced kinetic energy also decreases the severity of a crash and the numbers presented indicate clear significance of this. Hence, a lane-keeping ESC has double benefit since it will both increase the possibility of avoiding an accident by staying in lane, and decrease the severity of an accident if it should happen nevertheless.

REFERENCES

Åkesson, J., Årzén, K.E., Gäfvert, M., Bergdahl, T., and Tummescheit, H. (2010). Modeling and optimization with Optimica and JModelica.org—Languages and tools for solving large-scale dynamic optimization problems. *Computers and Chemical Engineering*, 34(11), 1737–1749.

Ali, M. (2012). *Decision Making and Control for Automotive Safety*. Ph.D. thesis, Chalmers University of Technology, Sweden. Thesis No. 3413.

Ali, M., Falcone, P., Olsson, C., and Sjöberg, J. (2013). Predictive prevention of loss of vehicle control for roadway departure avoidance. *IEEE Trans. Intell. Transp. Syst.*, 14(1), 56–68.

Andreasson, J. (2009). Enhancing active safety by extending controllability—How much can be gained? In *Proc. IEEE Intell. Vehicles Symp.*, 658–662. Xi'an, Shaanxi, China.

Benine-Neto, A. (2011). *Trajectory control in curves, towards the Perceptive-ESC, through a Piecewise Affine approach*. Ph.D. thesis, Université dEvry-Val-d'Essonne, France.

Berntorp, K. (2013). Derivation of a six degrees-of-freedom ground-vehicle model for automotive applications. Technical Report ISRN LUTFD2/TFRT--7627--SE, Department of Automatic Control, Lund University, Sweden.

Berntorp, K., Olofsson, B., Lundahl, K., Bernhardsson, B., and Nielsen, L. (2013). Models and methodology for optimal vehicle maneuvers applied to a hairpin turn. In *Proc. Am. Control Conf. (ACC)*, 2142–2149. Washington, DC.

Biegler, L.T., Cervantes, A.M., and Wächter, A. (2002). Advances in simultaneous strategies for dynamic process optimization. *Chemical Engineering Science*, 57, 575–593.

Bosch, R. (ed.) (2011). *Bosch Automotive Handbook*. Wiley, Hoboken, NJ, 8th edition.

Chakraborty, I., Tsiotras, P., and Diaz, R.S. (2013). Time-optimal vehicle posture control to mitigate unavoidable collisions using conventional control inputs. In *Proc. Am. Control Conf. (ACC)*, 2165–2170. Washington, DC.

Griewank, A. (2000). Evaluating derivatives: Principles and techniques of algorithmic differentiation. *Frontiers in Applied Mathematics, SIAM*, 19.

Isermann, R. (2006). *Fahrdynamik-Regelung: Modellbildung, Fahrerassistenzsysteme, Mechatronik*. Vieweg-Verlag, Wiesbaden, Germany.

Jansson, J. (2005). *Collision Avoidance Theory—with Application to Automotive Collision Mitigation*. Ph.D. thesis, Linköping University. Thesis No. 950.

Johansen, T.A. (2006). Adaptive optimizing dynamic control allocation algorithm for yaw stabilization of an automotive vehicle using brakes. In *Proc. 14th Mediterranean Conf. Control and Automation*. Ancona, Italy.

Kim, S.Y. and Oh, S.Y. (2003). A driver adaptive lane departure warning system based on image processing and a fuzzy evolutionary technique. In *Proc. IEEE Intelligent Vehicles Symp.*, 361–365. Columbus, OH.

Lundahl, K., Berntorp, K., Olofsson, B., Åslund, J., and Nielsen, L. (2013). Studying the influence of roll and pitch dynamics in optimal road-vehicle maneuvers. In *Proc. Int. Symp. Dynamics of Vehicles on Roads and Tracks (IAVSD)*. Qingdao, China.

Modelica Association (2014). URL: http://www.modelica.org.

Olofsson, B., Lundahl, K., Berntorp, K., and Nielsen, L. (2013). An investigation of optimal vehicle maneuvers for different road conditions. In *Proc. 7th IFAC Symp. Advances in Automotive Control (AAC)*. Tokyo, Japan.

Pacejka, H.B. (2006). *Tyre and Vehicle Dynamics*. Butterworth-Heinemann, Oxford, United Kingdom, 2nd edition.

Rajamani, R. (2006). *Vehicle Dynamics and Control*. Springer-Verlag, Berlin Heidelberg.

Sundström, P., Jonasson, M., Andreasson, J., Stensson Trigell, A., and Jacobsson, B. (2010). Path and control optimisation for over-actuated vehicles in two safety-critical maneuvers. In *Proc. 10th Int. Symp. Advanced Vehicle Control (AVEC)*. Loughborough, United Kingdom.

Tøndel, P. and Johansen, T.A. (2005). Control allocation for yaw stabilization in automotive vehicles using multiparametric nonlinear programming. In *Proc. Am. Control Conf. (ACC)*, 453–458. Portland, OR.

Wächter, A. and Biegler, L.T. (2006). On the implementation of an interior-point filter line-search algorithm for large-scale nonlinear programming. *Mathematical Programming*, 106(1), 25–57.